Chemokines direct endothelial progenitors into tumor neovessels

Herbert Spring*, Thomas Schüler†, Bernd Arnold†, Günter J. Hämmerling†, and Ruth Ganss†‡

*Biomedical Structure Analysis Group and †Department of Molecular Immunology, German Cancer Research Center, D-69120 Heidelberg, Germany

Tumor neovasculature substantially derives from sprouting of existing vessels, whereas the functional contribution of bone marrow-derived progenitors to neovessels remains controversial. We used transgenic mouse models of multistep carcinogenesis to monitor incorporation of bone marrow-derived cells into the neovasculature and to elucidate mechanisms of endothelial precursor cell (EPC) recruitment into the tumor microenvironment. We unequivocally demonstrate integration of bone marrow cells into the tumor vasculature as a late event in carcinogenesis that temporally correlates with VEGF release by the tumor and mobilization of circulating EPC in the periphery. Moreover, we demonstrate a chemokine-dependent mechanism of EPC homing into tumor, whereby neovessels of late-stage tumors release a battery of CC chemokines, which direct CCR2$^+$ and CCR5$^+$ progenitors into the vasculature. Thus, we show that tumor vessels promote their own growth and development in a self-amplifying fashion.

cancer | neovascularization

Neovascularization is essential for the growth of solid tumors (1). There is also accumulating evidence that circulating, bone marrow-derived progenitor cells incorporate into tumor-associated stroma to support carcinogenesis. However, the contribution of endothelial precursor cells (EPC) to tumor neovessels varies considerably among tumor models. Some experimental systems have demonstrated significant but variable integration of EPC (2–5), whereas in other models bone marrow-derived cells associate, but do not integrate, with endothelium and promote angiogenesis only indirectly (6–8). Whether EPC integrate into the vasculature, or are merely in close periendothelial association, remains controversial because analyses are based on histology and are limited by resolution. Moreover, it is unclear how circulating EPC home from the bone marrow specifically into the tumor microenvironment, and when during multistep tumorigenesis they are recruited into the preexisting vascular network. To address these questions we used transgenic mouse models of *de novo* tumorigenesis that mimic the clinical situation with regard to tissue tropism and growth kinetics. In rat insulin gene promoter 1 (RIP1)-SV40 large T antigen 5 (Tag5) mice the oncogene Tag is expressed under the control of RIP and tumors develop from hyperplastic and angiogenic islets to highly vascularized insulinomas by the age of 30 weeks (9). Similarly, in albumin-Tag (AlbTag) mice Tag oncogene is targeted to hepatocytes and drives tumor progression through hyperplasia, dysplasia, and eventually hepatocellular carcinoma by the age of 14–16 weeks (32). Neovascularization is a hallmark of carcinogenesis in both models of autochthonous tumor growth and comprises two distinct phases, initially an increase in vessel caliber in small nodules followed by extensive sprouting and loss of vessel hierarchy in late tumor stages (10). Moreover, vessel remodeling correlates with profound molecular changes in the tumor vasculature (11). Here we provide evidence that tumor-associated endothelium itself recruits progenitors into tumors, an effect mediated by chemokines acting through the cognate CC chemokine receptors expressed by circulating EPC.

Materials and Methods

Mice. RIP1-Tag5 mice on the C3H background were kindly provided by D. Hanahan (University of California, San Francisco). AlbTag mice were generated by expressing Tag under the control of the Alb promoter/enhancer and backcrossed into the C3HeBFe background for 20 generations (32). Enhanced GFP (EGFP) reporter mice were generated by knock-in of the EGFP gene in the murine locus for the receptor for advanced glycated end products (RAGE). Ubiquitous deletion of exons 2–7 of the RAGE gene moves the thymidine kinase promoter directly in front of the start site of the EGFP gene and activates transcription (12). In tie2Cre×EGFP mice Cre recombinase is exclusively expressed in endothelial cells and activates EGFP transcription by deleting parts of the RAGE gene (12). RIP1-Tag5 and AlbTag mice were lethally irradiated (10 Gy) at the age of 6 and 4 weeks, respectively, and reconstituted with 2×10^6 EGFP$^+$, unfractionated bone marrow cells. To monitor bone marrow reconstitution, peripheral blood monocytes were stained with phycoerythrin-labeled anti-CD8 (53-6.7, rat IgG2a, 2.5 μg/μl), anti-B220 (RA3-6B2, rat IgG2a, 5 μg/μl), and anti-CD11b (M1/70, rat IgG2b, 5 μg/ml) antibodies and analyzed by FACS. Antibodies were purchased from BD Pharmingen. All experimental protocols were approved by the Animal Welfare Board of the Regierungspräsidium (Karlsruhe, Germany).

Histological Analysis and Confocal Laser Scanning Microscopy. Mice were injected i.v. with 100 μg of tetramethylrhodamine isothiocyanate (TRITC)-labeled tomato lectin (*Lycopersicon esculentum*, Sigma, Taufkirchen, Germany). After 10 min of circulation, mice were heart-perfused with PBS followed by 4% paraformaldehyde (PFA) in PBS. Organs were postfixed for 2–6 h in PFA and overnight in 30% sucrose. Ten- to 30-μm frozen sections were analyzed. For confocal microscopy a LSM 510 UV microscope (Zeiss) with plan-Neofluar objectives ×20/0.8 and ×40/1.3 oil and laser lines of 488-nm wavelength for GFP and 543-nm wavelength for TRITC-lectin detection was used. Images were processed by using PHOTOSHOP 5.5 (Adobe Systems, San Jose, CA).

Cell Isolation and FACS. Small RIP1-Tag5 tumors were isolated under a dissecting microscope after collagenase digestion of pancreatic tissue as described in ref. 11. Macroscopically visible solid tumors were dissected from pancreatic tissue with scissors. Purification of endothelial cells from RIP1-Tag5 tumors was described in ref. 11. Endothelial cells from normal liver and

MEDICAL SCIENCES

AlbTag tumors were isolated following a protocol by Knolle *et al.* (13). For FACS staining, cells were incubated with Fc block (CD16/CD32, 2.4G2, 2.5 $\mu g/\mu l$; BD Pharmingen) and specifically labeled with anti-CD31-phycoerythrin (MEC 13.3, rat IgG2a, 4 $\mu g/ml$; BD) and ME-9F1-biotin (rat IgG2a, 30 $\mu g/ml$) (14), followed by incubation with streptavidin Red 670 (1:300, Invitrogen). Cells were analyzed on a FACScan (Becton Dickinson, Heidelberg, Germany) or sorted by using a FACSVantage SE flow cytometer (Becton Dickinson). Tumor-infiltrating lymphocytes (TIL) were prepared as described for endothelial cells but were separated on a Percoll gradient.

ELISA. Serum was collected from AlbTag mice at different stages during tumor progression. ELISA were performed according to the manufacturer's instructions for mouse MCP-1/CCL2 (BD OptEIA Set, BD Biosciences), mouse MIP-1α/CCL3, mouse RANTES/CCL5, mouse stromal-derived factor 1/CXCL12, mouse VEGF (all DuoSet, R & D Systems), and mouse placental growth factor 2 (PlGF-2) (Quantikine M, R & D Systems) and measured by Multiskan Ascent (Labsystems, Helsinki).

Quantitative RT-PCR Analysis. Quantitative RT-PCR was performed using by real-time PCR TaqMan technology (Applied Biosystems) as described in ref. 11. The mouse hypoxanthine phosphoribosyltransferase (*Hprt*) gene served as an internal control.

***Ex Vivo* Expansion of EPC.** Mice were i.v. injected once with 2×10^8 infectious units (ifu) of adenovirus without transgene (ΔAd) or adenovirus expressing mVEGF$_{165}$, or with 1×10^7 ifu of adenoviruses expressing mCCL2 or mCCL3. AdVEGF$_{165}$, AdCCL2, and AdCCL3 viruses were obtained by cloning full-length cDNA encoding the corresponding genes into the pShuttleCMV transfer vector followed by homologous recombination with pAdEasy-1 and virus production in 293 cells according to the instructions of the AdEasy Vector System (Quantum Biotechnologies, Montreal, Canada). Mice were killed 3 days after the last injection. Mononuclear cells from spleen were isolated by density-gradient centrifugation (15). A total of 2×10^6 cells per cm^2 were seeded on human fibronectin (Falcon)-coated glass slides in 24-well plates and cultured for 3 days in EndoCult medium (CellSystems, St. Katharinen, Germany). On day 3, wells were incubated with 200 $\mu g/ml$ 1,1'-dioctadecyl-3,3,3',3',-tetramethylindocarbocyanine (DiI)-labeled acetylated low-density lipoprotein (DiI-Ac-LDL, Paesel & Lorei, Hanau, Germany) for 2 h, and cells were fixed in 4% paraformaldehyde, permeabilized with methanol, and stained with anti-CD31 antibodies (BD Pharmingen). Dual staining, early outgrowth endothelial colonies (16) were identified and counted under a fluorescent Axioplan 2 microscope (Zeiss). For FACS analysis, cells were stained with mouse CCL2 biotin conjugate (Fluorokine kit, R & D Systems) or biotinylated anti-CCR5 (C34/3448, rat IgG2c, 0.25 $\mu g/ml$, BD Pharmingen). For adoptive transfers of *ex vivo*-expanded EPC, C3H "green" bone marrow chimeras were injected with 2×10^8 ifu of AdVEGF$_{165}$ virus and killed on day 3. Mononuclear splenic cells were seeded on fibronectin-coated six-well plates and grown for 5 days. Green cells positive for DiI-Ac-LDL were sorted by using a FACSVantage SE flow cytometer (Becton Dickinson). Some sorted EPC were incubated in medium containing 100 ng/ml pertussis toxin (PTX, Alexis, Grünberg, Germany) for 1 h in a 37°C tissue culture incubator and washed twice in PBS. To assess viability, control cells were plated on fibronectin, and DiI-Ac-LDL-positive cells were monitored. A total of 1×10^6 cells were reinjected into tumor-bearing AlbTag mice.
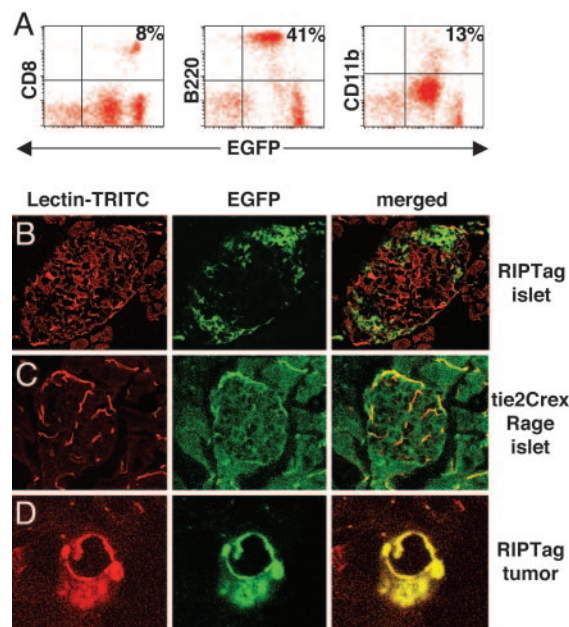

Fig. 1. Incorporation of EGFP$^+$ bone marrow-derived cells during RIP1-Tag5 tumorigenesis. (*A*) Representative FACS blots demonstrating multilineage reconstitution (CD8$^+$ T cells, B220$^+$ B cells, and CD11b$^+$ monocytes/macrophages) 4 weeks after bone marrow transplantation in recipient RIP1-Tag5 mice. Bone marrow was derived from EGFP reporter mice that ubiquitously express EGFP. Peripheral blood analysis of EGFP$^+$ donor mice results in similar leukocyte frequencies (data not shown). (*B*) Hyperplastic islets from 16-week-old RIP1-Tag5 mice, reconstituted with EGFP$^+$ bone marrow at 6 weeks, display infiltrating immune cells (green) that do not overlap with the lectin-perfused microvasculature (red). (*C*) In contrast, tie2Cre×Rage mice are genetically engineered to express EGFP in all vessels, and overlapping EGFP$^+$ (green) and lectin-perfused (red) vessels in an islet of Langerhans are depicted. (*D*) EGFP$^+$ vessels are detectable in insulinoma from 30-week-old RIP1-Tag5 bone marrow chimeras. (Magnifications: *B* and *C*, ×25; *D*, ×40.)

Results

Bone Marrow-Derived EPC Integrate into Late-Stage Tumors but Not Early Tumor Lesions. To monitor the recruitment of bone marrow-derived cells during distinct phases of vessel remodeling, 6-week-old RIP1-Tag5 mice were lethally irradiated and reconstituted with EGFP-expressing bone marrow cells derived from an EGFP reporter mouse (12). Complete multilineage reconstitution 4 weeks after bone marrow transplant in transgenic recipients was confirmed by FACS analysis (Fig. 1*A*). Early and advanced tumors were subsequently analyzed for colocalization of GFP with lectin-perfused vessels. Early tumor stages in 16-week-old RIP1-Tag5 mice, called hyperplastic islets, are infiltrated by bone marrow-derived EGFP$^+$ leukocytes consistent with an anti-Tag autoimmune response (9), although the infiltrating cells are discrete and separate from microvessels (Fig. 1*B*). This finding clearly contrasts with control mice (tie2Cre×Rage), where EGFP is specifically expressed in all vessels, including those of normal endocrine and exocrine pancreas (12) (Fig. 1*C*). Most important, however, in late-stage insulinomas (30-week-old mice), parts of the vasculature are EGFP-positive, indicating that bone marrow-derived endothelial cells have integrated with tumor neovessels (Fig. 1*D*). To compare these results with a different model of multistep tumor progression resulting in hepatocellular carcinoma, AlbTag mice were reconstituted with bone marrow cells from the EGFP reporter mouse at 4 weeks of age. Subsequent histological analyses in AlbTag livers shows that early nodular carcinomas in 8-week-old mice do not integrate EGFP$^+$ bone marrow-derived cells (data not shown), whereas, in advanced hepatocellular carcinomas of 16-week-old mice, bone
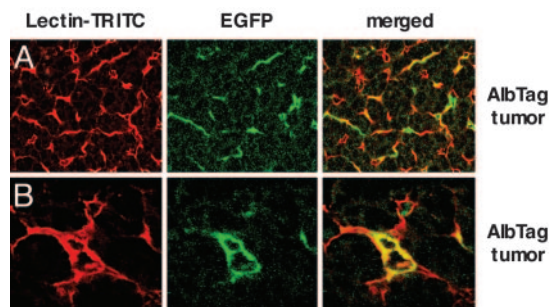
Fig. 2. Incorporation of EGFP+ bone marrow-derived cells into AlbTag neovessels. (*A*) Overview of the tumor microvasculature of a 14-week-old AlbTag mouse, reconstituted with bone marrow from an EGFP reporter mouse at the age of 4 weeks. Bone marrow-derived EGFP+ green cells are homogeneously distributed. (*B*) EGFP+ bone marrow-derived cells overlap with red liver tumor vessels. (Magnifications: *A*, ×25; *B*, ×40.)

marrow-derived cells substantially contribute to neovessels, as shown by homogeneous scattering of green endothelial cells throughout the tumor (Fig. 2). Thus, because of integration with neovessels, bone marrow-derived cells are detectable in autochthonous tumors during late phases of tumorigenesis.

Quantification of Bone Marrow-Derived Endothelial Cells During Tumor Progression. To complement our histological data, we used a combination of vessel-specific antibodies and FACS analysis to distinguish endothelia from neighboring cells (11) (Fig. 3*A*). Endothelial cells were isolated by enzymatic tissue dissociation, enriched by gradient centrifugation, and labeled with the endothelial cell-specific antibodies CD31 and ME-9F1 (14). Cells with the highest fluorescence for both markers have been shown to represent a highly purified endothelial cell fraction (11). Isolation of endothelial cells by FACS allowed us to determine the relative abundance of bone marrow-derived EGFP+ cells within the endothelial cell population during multistep tumorigenesis. As controls, endothelial cells purified from normal liver of wild-type bone marrow chimeras (C3H) display a background green fluorescence of only 2% compared with 90% in tie2Cre×Rage livers, where EGFP is specifically expressed by all endothelial cells (Fig. 3*B*), thus validating our purification technique. In early tumors of 10-week-old AlbTag mice, EGFP+ endothelial cells are not detectable by FACS, indicating that bone marrow cells do not contribute to early tumorigenesis. This finding is consistent with our histology data. However, the frequency of EGFP+ endothelial cells increases with tumor progression, being 5.8 ± 0.8% at 12 weeks, 14.3 ± 1.7% at 14 weeks, and 26.8 ± 4.1% of endothelial cells at 16 weeks (late-stage tumors, Fig. 3*C*). Small, only microscopically detectable tumors in 20-week-old RIP1-Tag5 mice display 15% bone marrow-derived EGFP+ cells in the vessel fraction (Fig. 3*C*). The number of EGFP+ endothelial cells increases dramatically in RIP1-Tag5 late-stage insulinomas at week 32, where they represent ≈38% of all tumor endothelial cells (Fig. 3*C*). Thus, a substantial number of bone marrow-derived EPC predominantly contribute to later stages of vessel remodeling, when extensive vessel sprouting occurs (10). Moreover, these data are consistent in two independent models of carcinogenesis.

Release of CC Chemokines by Tumor Endothelial Cells Correlates with Cognate Receptor Expression by EPC. The mobilization of EPC from the bone marrow into the bloodstream, migration to the tumor site, and subsequent integration into the vascular network are all presumably controlled by tumor-derived factors. VEGF, for instance, plays an exquisite role in mobilizing EPC and hematopoietic stem cells from the bone marrow (16, 17), a
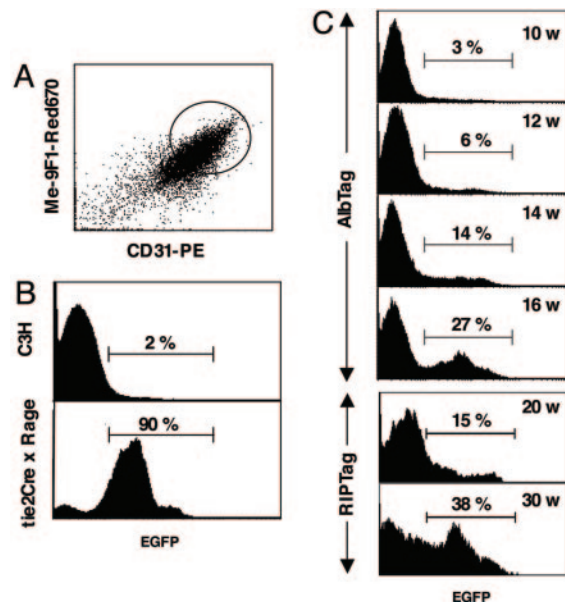
Fig. 3. Quantification of bone marrow-derived endothelial cells during multistep tumor progression. (*A*) Endothelial cells were freshly isolated from normal or cancerous tissue of EGFP bone marrow chimeras after enzymatic digestion and density-gradient centrifugation. CD31 and ME-9F1 double-positive cells that represent endothelial cells were gated, and the number of EGFP+ cells was quantified by FACS. (*B*) C3H wild-type mice reconstituted with EGFP+ bone marrow display a background green fluorescence intensity of 2%. Tie2Cre×Rage mice are genetically engineered to express EGFP+ in all vessels and serve as control. Ninety percent of liver endothelial cells isolated from tie2Cre×Rage mice are green. (*C*) The percentage of EGFP+ cells in purified LTEC was monitored throughout tumor progression in AlbTag EGFP+ bone marrow chimeras of 10, 12, 14, and 16 weeks of age. It is technically not feasible to purify endothelial cells from early hyperplastic stages in RIP1-Tag5 mice; however, endothelial cells from angiogenic islets/small tumors (at 20 weeks of age) and end-stage tumors of 32-week-old RIP1-Tag5 chimeras were analyzed, and EGFP+ cells were quantified. Six to 10 mice per group were analyzed.

function that can be inhibited by VEGF-specific antibodies (18). However, mechanisms regulating EPC recruitment from the circulation into the tumor are not yet understood. Interestingly, gene profiling of liver tumor-derived endothelial cells revealed expression of CC chemokines such as CCL2, CCL3, CCL4, CCL5, CCL7, and CCL8 specifically in the tumor vasculature, suggesting an important role during neovascularization (32). Moreover, we shown here that CCL2, CCL3, and CCL5 are released into the circulation of tumor-bearing AlbTag mice over time (Fig. 4*A*). Strikingly, these chemokines are exclusively produced by tumor endothelial cells but not by other tumor constituents such as tumor cells or TIL (Fig. 4*B*). To assess the potential of chemokines to activate endothelial progenitors, we analyzed expression of the CC chemokine receptors CCR2 and CCR5, the cognate receptors for CCL2 and CCL3/CCL5, respectively, on EPC and tumor endothelial cells (Fig. 4 *C* and *D*). Interestingly, peripheral EPC display the highest expression of chemokine receptors, with ≈44% of EPC being positive for CCR2 and 11% being positive for CCR5 (Fig. 4*D*), a finding that correlates CC chemokine receptor expression with migratory capacity. Moreover, EPC-derived liver tumor endothelial cells (LTEC) isolated from AlbTag EGFP bone marrow chimeras (EGFP+ green LTEC) can still be distinguished from native tumor LTEC by differential expression of chemokine receptors (Fig. 4*D*).

EPC Mobilization from Bone Marrow Correlates with VEGF Secretion. Mobilization of VEGFR2+ EPC from the bone marrow into the circulation represents the first critical step for EPC recruitment.

Fig. 4. Chemokine secretion by LTEC. (*A*) CCL2, CCL3, and CCL5 serum levels were quantified during tumor progression in 6- to 16-week-old AlbTag mice by ELISA. Four to 15 mice were analyzed per age group. ∗, $P < 0.05$ compared with 6-week-old AlbTag mice (Mann–Whitney test). (*B*) AlbTag tumor constituents such as TIL, hepatoma cells (Tumor), and LTEC were isolated, and CC chemokine secretion was assessed by ELISA from 2-day culture supernatant. Experiments were performed in triplicate, and a summ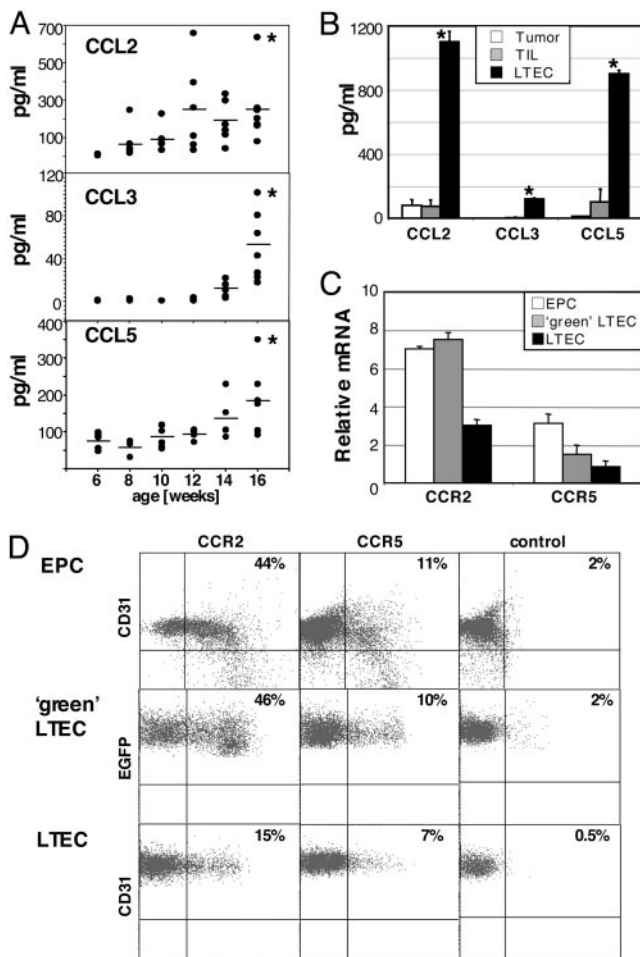ary of three independent experiments is shown. ∗, $P < 0.01$ versus TIL. (*C*) VEGF-mobilized EPC were expanded *in vitro* in endothelial growth medium. LTEC from 16-week-old AlbTag bone marrow chimeras were isolated and separated by FACS into EGFP$^+$ bone marrow-derived (green LTEC) and non-green endothelial (LTEC) fractions. Expression of the CC chemokine receptors CCR2 and CCR5 was assessed by quantitative RT-PCR. Three independent samples were analyzed and normalized against hypoxanthine phosphoribosyltransferase. (*D*) Binding of biotinylated CCL2 on *ex vivo*-expanded EPC (also stained with CD31-phycoerythrin) and fractionated EGFP$^+$ LTEC (double-positive for ME-9F1 and CD31) and EGFP$^-$ LTEC (double-positive for ME-9F1 and CD31) indicates functional CCR2 receptor expression. CCR5 receptor expression on EPC and LTEC populations was analyzed by FACS by using monoclonal antibodies. Isotype controls for CCR5 are shown.

Various growth factors have been implicated in the mobilization of EPC from the bone marrow, including VEGF (16, 17), stromal derived factor 1 (SDF-1/CXCL12) (19), and PlGF (20). In AlbTag mice we found that VEGF is secreted by tumor cells (data not shown) and serum levels positively correlate with tumor size, consistent with its crucial role during tumor angiogenesis (Fig. 5*A*). In contrast, peripheral CXCL12 and PlGF levels are not significantly elevated in tumor-bearing animals (Fig. 5*A*). Because CCL2, CCL3, and CCL5 are released by tumor endothelial cells during tumorigenesis and CCR2$^+$ and CCR5$^+$ EPC are potentially responsive to chemokine signaling,

we next aimed to clarify the role of CC chemokine signaling for EPC mobilization from bone marrow. Consistent with VEGF secretion during tumorigenesis, elevated plasma VEGF concentrations in AlbTag mice with advanced tumors or in Ad-VEGF$_{165}$-treated wild-type mice increase circulating EPC as monitored at day 3 after viral injection (Fig. 5*B*). In contrast, administration of adenoviruses expressing CCL2 or CCL3 *in vivo* does not increase the numbers of circulating EPC (Fig. 5*B*), indicating a less prominent role of chemokines in EPC mobilization from the bone marrow.

Endothelial CC Chemokines Direct EPC into the Vascular Bed. Mobilization of EPC from bone marrow and homing into tumors are two important but independent events. To assess a potential role of CC chemokines in directing EPC into the tumor environment, we monitored migration of adoptively transferred, *ex vivo*-expanded EPC into AlbTag tumors. Because chemokine receptors signal via G protein-mediated receptors, we also investigated the *in vivo* homing capacity of adoptively transferred EPC treated with PTX, an inhibitor of chemokine receptor signaling (21). EPC were derived from C3H green bone marrow chimeras after VEGF mobilization and expanded *ex vivo*. The majority of these EGFP$^+$ cells were also metabolically labeled with DiI-Ac-LDL (55–65%, Fig. 6*A*), confirming a bone marrow-derived endothelial cell phenotype. Purified double-positive cells were either left untreated or incubated with PTX, which does not impair viability (Fig. 6*B*). Upon transfer into 12- to 14-week-old AlbTag mice with rapidly expanding tumors, *ex vivo*-derived, non-PTX-treated EPC integrate into tumor vessels. After 7 days, $9.7 \pm 2\%$ green cells are incorporated into the tumor vasculature as shown by FACS analysis (Fig. 6*C*). In striking contrast, PTX treatment abrogates homing of green endothelial precursors into AlbTag tumors ($1.3 \pm 1\%$), thus suggesting a crucial role for chemokine receptor signaling in the recruitment of bone marrow-derived cells during tumor angiogenesis (Fig. 6*C*).

Discussion

Tumor neovascularization is a precisely coordinated process characterized by vessel dilation in the early phases and extensive vessel sprouting in rapidly growing tumors (10). Here we conclusively show with two independent mouse models that only advanced tumors recruit and incorporate bone marrow-derived EPC into neovessels, possibly to further compensate for escalating oxygen and nutrient requirements. Approximately 30–40% of green endothelial cells are found throughout liver and pancreatic tumors, and their homogeneous scattering indicates evenly distributed EPC recruitment instead of accumulation at "hotspots" of neovascularization. Because our study demonstrates that EPC incorporation is a late event in carcinogenesis, the relative contribution of bone marrow-derived endothelial cells to tumor neovessels will vary depending on tumor size and degree of neovascularization. Moreover, our findings imply that therapeutic tumor targeting by EPC will predominantly affect late-stage tumors and may require combination with other, earlier-acting modalities.

Until now, molecular mechanisms underlying the homing of bone marrow-derived endothelial progenitors into tumors were unknown. Here we have identified key factors that sequentially regulate the integration of bone marrow-derived endothelial cells into liver tumor neovasculature. During AlbTag carcinogenesis, VEGF is secreted by tumor cells into the circulation, which then mobilizes endothelial progenitors from the bone marrow. This finding is consistent with previous findings that release of hematopoietic stem cells from bone marrow crucially involves VEGF (2, 17, 22, 23). Furthermore, during angiogenesis tumor-resident endothelial cells acquire new characteristics, which include the overexpression of CC chemokines. These growth factors are subsequently released into the circulation,
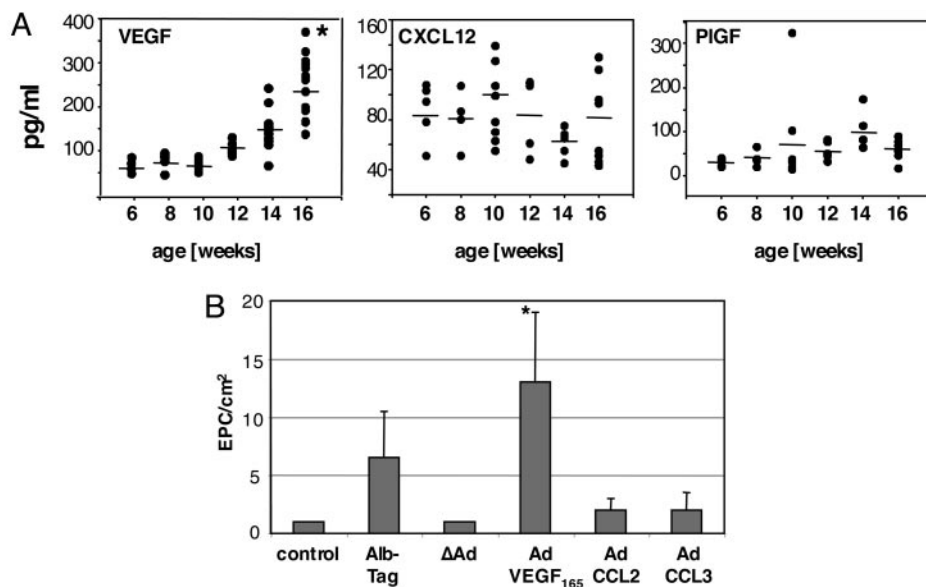
Fig. 5. Elevated VEGF plasma levels correlate with EPC mobilization from bone marrow. (*A*) VEGF, CXCL12, and PlGF serum levels were quantified during tumor progression in 6- to 16-week-old AlbTag mice by ELISA. Four to 15 mice were analyzed per age group. ∗, $P < 0.01$ compared with 6-week-old AlbTag mice; CXCL12 and PlGF serum elevation during tumorigenesis was statistically not significant. (*B*) C3H control mice were left untreated; AlbTag mice represent 16-week-old mice with late-stage tumors. C3H mice were i.v. injected with 2×10^8 ifu of ''empty'' adenovirus (ΔAd), 2×10^8 ifu of adenovirus expressing mVEGF$_{165}$ (AdVEGF$_{165}$, VEGF plasma level of 500–700 pg/ml), 1×10^7 ifu of adenovirus-expressing CCL2 (AdCLL2, CCL2 plasma level of 300–600 pg/ml), or 1×10^7 ifu of adenovirus-expressing CCL3 (AdCLL3, CCL3 plasma level of 100–300 pg/ml). Mononuclear cells were isolated from spleen, and EPC colonies were identified by CD31 immunostaining and metabolic labeling with DiI-Ac-LDL after 3 days in culture and quantified by using fluorescent microscopy ($n = 3$ per group, mean ± SD; ∗, $P = 0.01$ versus control).

where they guide progenitor cells, which express high levels of the corresponding CC chemokine receptors, into the tumor bed. Thus, during tumor formation, preexisting endothelial cells and

Fig. 6. Chemokine signaling is crucially involved in EPC homing into AlbTag tumors. (*A*) Before adoptive transfer, EGFP$^+$ EPC derived from VEGF-mobilized C3H bone marrow chimeras were metabolically labeled with DiI-Ac-LDL, and double-positive cells were sorted by FACS. (*B*) Sorted EPC were left untreated (−PTX) or were treated with PTX (+PTX), and the viability of replated monolayers was assessed by uptake of DiI-Ac-LDL. (Magnification: ×40.) (*C*) A total of 1×10^6 untreated EGFP$^+$ (−PTX) or PTX-treated (+PTC) EPC were adoptively transferred in 12-week-old AlbTag mice. Seven days later endothelial cells were isolated from solid tumors, and the percentage of green CD31$^+$, ME-9F1$^+$ endothelial cells was analyzed by FACS ($n = 3$ per group).

recruited progenitors promote neovascularization in a self-amplifying loop.

CC chemokines are classically known to attract leukocytes to sites of inflammation. In AlbTag mice, however, lymphocyte migration into liver parenchyma is attenuated, suggesting a different role for chemokines during liver carcinogenesis (32). It is particularly intriguing that liver endothelial cells secrete CC chemokines and also express their cognate receptors. Moreover, circulating EPC and recently recruited endothelial cells display the highest receptor expression, which may correlate with their enhanced capacity to respond to chemokine sources. There is precedence for CCR2 and CCR5 expression on some mature vascular cells (24–26), and recombinant CCL2 induces migration of human umbilical vein endothelial cells in a dose-dependent manner. Similarly, CCL2 mediates chemoattraction and transmigration of EPC *in vitro* (27). However, in this study we report on functional CCR2 and CCR5 expression on EPC. Because liver endothelial cells release a battery of different CC chemokines, it is possible that other CC chemokines also play a role in EPC homing into tumor tissue. Remarkably, it is not the tumor itself, but endothelial cells as components of the tumor-induced stroma, which recruit EPC. Recently, it has been demonstrated that human breast carcinoma uses tumor-induced fibroblasts to recruit EPC through secretion of the CXC chemokine CXCL12 (19). Although EPC are strongly positive for the corresponding receptor, CXCR4, we have no evidence for increased CXCL12 expression during AlbTag carcinogenesis, and, indeed, tumor endothelial cells are biased to produce CC chemokines.

Chemokines released by tumor endothelial cells may not only attract EPC to the tumor site but may also promote firm adhesion of EPC to neovessels. This support of adhesion has been shown for CXCR4-CXCL12 interactions, which cause firm adhesion of previously rolling CD34$^+$ progenitors (28). At the tumor site, several adhesion molecules may act synergistically to control EPC integration. E- and P-selectins, for instance, mediate initial arrest of embryonic EPC during tumor angiogenesis (29). Indeed, we have preliminary evidence in AlbTag mice that

blocking E- and P-selectin signaling *in vivo* prevents incorporation of green bone marrow-derived endothelial cells into tumor vessels. Furthermore, during hind limb ischemia, β2 integrins are involved in homing and integration of progenitor cells into sites of ischemia (27), and in subsequent steps cysteine proteases like cathepsin L facilitate invasion of stem cells (30). Thus, postnatal neovascularization is a complex process that requires a highly coordinated sequence of multiple receptor–ligand interactions to recruit and functionally incorporate EPC.

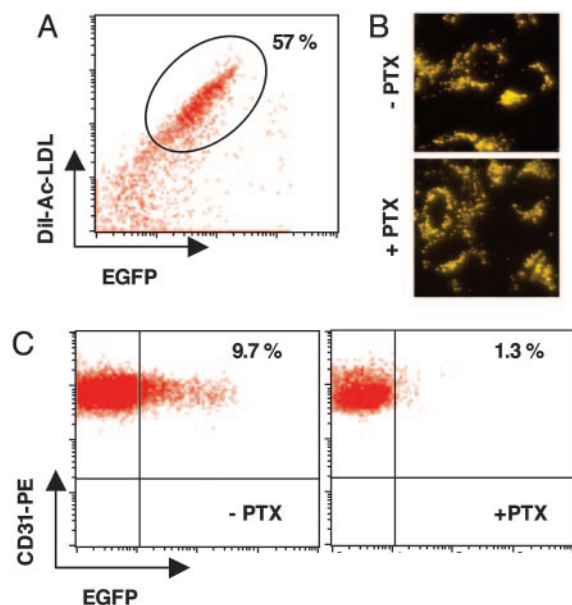Our strategy to separate newly incorporated from preexisting tumor endothelial cells unequivocally proves the contribution of bone marrow cells to the neovasculature. However, bone marrow also contributes to other tumor stromal components, e.g., mononuclear infiltrating cells (2, 6), periendothelial mural cells (7),

myofibroblasts, and fibroblasts (19, 31), which may all indirectly affect neovascularization and tumor progression. Because the stromal composition and local cytokine/chemokine milieu may vary depending on tumor type and location (3, 4), recruitment of bone marrow cells into tumors might be highly tumor- and stage-specific, which has important therapeutic implications.

1. Hanahan, D. & Folkman, J. (1996) *Cell* **86,** 353–364.
2. Lyden, D., Hattori, K., Dias, S., Costa, C., Blaikie, P., Butros, L., Chadburn, A., Heissig, B., Marks, W., Witte, L., *et al.* (2001) *Nat. Med.* **7,** 1194–1201.
3. Ruzinova, M. B., Schoer, R. A., Gerald, W., Egan, J. E., Pandolfi, P. P., Rafii, S., Manova, K., Mittal, V. & Benezra, R. (2003) *Cancer Cell* **4,** 277–289.
4. Li, H., Gerald, W. L. & Benezra, R. (2004) *Cancer Res.* **64,** 6137–6143.
5. Hilbe, W., Dirnhofer, S., Oberwasserlechner, F., Schmid, T., Gunsilius, E., Hilbe, G., Woll, E. & Kahler, C. M. (2004) *J. Clin. Pathol.* **57,** 965–969.
6. De Palma, M., Venneri, M. A., Roca, C. & Naldini, L. (2003) *Nat. Med.* **9,** 789–795.
7. Rajantie, I., Ilmonen, M., Alminaite, A., Ozerdem, U., Alitalo, K. & Salven, P. (2004) *Blood* **104,** 2084–2086.
8. Ziegelhoeffer, T., Fernandez, B., Kostin, S., Heil, M., Voswinckel, R., Helisch, A. & Schaper, W. (2004) *Circ. Res.* **94,** 230–238.
9. Ganss, R. & Hanahan, D. (1998) *Cancer Res.* **58,** 4673–4681.
10. Ryschich, E., Schmidt, J., Hammerling, G. J., Klar, E. & Ganss, R. (2002) *Int. J. Cancer* **97,** 719–725.
11. Berger, M., Bergers, G., Arnold, B., Hammerling, G. J. & Ganss, R. (2005) *Blood* **105,** 1094–1101.
12. Constien, R., Forde, A., Liliensiek, B., Grone, H. J., Nawroth, P., Hammerling, G. & Arnold, B. (2001) *Genesis* **30,** 36–44.
13. Knolle, P. A., Uhrig, A., Hegenbarth, S., Loser, E., Schmitt, E., Gerken, G. & Lohse, A. W. (1998) *Clin. Exp. Immunol.* **114,** 427–433.
14. Harder, R., Uhlig, H., Kashan, A., Schutt, B., Duijvestijn, A., Butcher, E. C., Thiele, H. G. & Hamann, A. (1991) *Exp. Cell Res.* **197,** 259–267.
15. Dimmeler, S., Aicher, A., Vasa, M., Mildner-Rihm, C., Adler, K., Tiemann, M., Rutten, H., Fichtlscherer, S., Martin, H. & Zeiher, A. M. (2001) *J. Clin. Invest.* **108,** 391–397.
16. Hattori, K., Dias, S., Heissig, B., Hackett, N. R., Lyden, D., Tateno, M., Hicklin, D. J., Zhu, Z., Witte, L., Crystal, R. G., *et al.* (2001) *J. Exp. Med.* **193,** 1005–1014.
17. Asahara, T., Takahashi, T., Masuda, H., Kalka, C., Chen, D., Iwaguro, H., Inai, Y., Silver, M. & Isner, J. M. (1999) *EMBO J.* **18,** 3964–3972.
18. Willett, C. G., Boucher, Y., di Tomaso, E., Duda, D. G., Munn, L. L., Tong, R. T., Chung, D. C., Sahani, D. V., Kalva, S. P., Kozin, S. V., *et al.* (2004) *Nat. Med.* **10,** 145–147.
19. Orimo, A., Gupta, P. B., Sgroi, D. C., Arenzana-Seisdedos, F., Delaunay, T., Naeem, R., Carey, V. J., Richardson, A. J. & Weinberg, R. A. (2005) *Cell* **121,** 335–348.
20. Hattori, K., Heissig, B., Wu, Y., Dias, S., Tejada, R., Ferris, B., Hicklin, D. J., Zhu, Z., Bohlen, P., Witte, L., *et al.* (2002) *Nat. Med.* **8,** 841–849.
21. Aiuti, A., Webb, I. J., Bleul, C., Springer, T. & Gutierrez-Ramos, J. C. (1997) *J. Exp. Med.* **185,** 111–120.
22. Heissig, B., Hattori, K., Dias, S., Friedrich, M., Ferris, B., Hackett, N. R., Crystal, R. G., Besmer, P., Lyden, D., Moore, M. A., *et al.* (2002) *Cell* **109,** 625–637.
23. Aicher, A., Heeschen, C., Mildner-Rihm, C., Urbich, C., Ihling, C., Technau-Ihling, K., Zeiher, A. M. & Dimmeler, S. (2003) *Nat. Med.* **9,** 1370–1376.
24. Weber, K. S., Nelson, P. J., Grone, H. J. & Weber, C. (1999) *Arterioscler. Thromb. Vasc. Biol.* **19,** 2085–2093.
25. Salcedo, R., Ponce, M. L., Young, H. A., Wasserman, K., Ward, J. M., Kleinman, H. K., Oppenheim, J. J. & Murphy, W. J. (2000) *Blood* **96,** 34–40.
26. Andjelkovic, A. V. & Pachter, J. S. (2000) *J. Neurochem.* **75,** 1898–1906.
27. Chavakis, E., Aicher, A., Heeschen, C., Sasaki, K., Kaiser, R., El Makhfi, N., Urbich, C., Peters, T., Scharffetter-Kochanek, K., Zeiher, A. M., *et al.* (2005) *J. Exp. Med.* **201,** 63–72.
28. Peled, A., Grabovsky, V., Habler, L., Sandbank, J., Arenzana-Seisdedos, F., Petit, I., Ben-Hur, H., Lapidot, T. & Alon, R. (1999) *J. Clin. Invest.* **104,** 1199–1211.
29. Vajkoczy, P., Blum, S., Lamparter, M., Mailhammer, R., Erber, R., Engelhardt, B., Vestweber, D. & Hatzopoulos, A. K. (2003) *J. Exp. Med.* **197,** 1755–1765.
30. Urbich, C., Heeschen, C., Aicher, A., Sasaki, K., Bruhl, T., Farhadi, M. R., Vajkoczy, P., Hofmann, W. K., Peters, C., Pennacchio, L. A., *et al.* (2005) *Nat. Med.* **11,** 206–213.
31. Direkze, N. C., Hodivala-Dilke, K., Jeffery, R., Hunt, T., Poulsom, R., Oukrif, D., Alison, M. R. & Wright, N. A. (2004) *Cancer Res.* **64,** 8492–8495.
32. Ryschich, E., Lizdenis, P., Ittrich, C., Benner, A., Stahl, S., Hamann, A., Schmidt, J., Knolle, P., Arnold, B., Hämmerling, G. J. & Ganss, R. *Cancer Res.*, in press.